TRAVEL TIME SIMULATION OF RADIONUCLIDES IN A 200 M DEEP HETEROGENEOUS CLAY FORMATION LOCALLY DISTURBED BY EXCAVATION

MARIJKE HUYSMANS[1], ARNE BERCKMANS[2] and ALAIN DASSARGUES[1,3]

[1]*Hydrogeology and Engineering Geology Group, Department of Geology-Geography, Katholieke Universiteit Leuven, Redingenstraat 16, 3000 Leuven, Belgium*

[2]*NIRAS/ONDRAF: Belgian Agency for Radioactive Waste and Enriched Fissile materials, Kunstlaan 14, 1210 Brussel, Belgium*

[3]*Hydrogeology, Department of Georesources, Geotechnologies and Building Materials, Université de Liège, Chemin des Chevreuils 1, Belgium*

Abstract. In Belgium, the Boom Clay Formation at a depth of 200 m below surface is being evaluated as a potential host formation for the disposal of vitrified nuclear waste. The aim of this study is to model the transport of radionuclides through the clay, taking into account the geological heterogeneity and the excavation induced fractures around the galleries in which the waste will be stored. This is achieved by combining a transport model with geostatistical techniques used to simulate the geological heterogeneity and fractures of the host rock formation. Two different geostatistical methods to calculate the spatially variable hydraulic conductivity of the clay are compared. In the first approach, one dimensional direct sequential co-simulations of hydraulic conductivity are generated, using measurements of hydraulic conductivity (K) and 4 types of secondary variables: resistivity logs, gamma ray logs, grain size measurements and descriptions of the lithology, all measured in one borehole. In the second approach, three dimensional cokriging was performed, using hydraulic conductivity measurements, gamma ray and resistivity logs from the same borehole and a gamma ray log from a second borehole at a distance of approximately 2000 m from the first borehole. For both methods, simulations of the fractures around the excavation are generated based on information about the extent, orientation, spacing and aperture of excavation induced fractures, measured around similar underground galleries. Subsequently, the obtained 3D cokriged and 1D simulated values of hydraulic conductivity are each randomly combined with the simulated fractures and used as input for a transport model that calculates the transport by advection, diffusion, dispersion, adsorption and decay through the clay formation. This results in breakthrough curves of the radionuclide Tc-99 in the aquifers surrounding the Boom Clay that reflect the uncertainty of travel time through the clay. The breakthrough curves serve as a risk management tool in the evaluation of the suitability of the Boom Clay Formation as a host rock for vitrified nuclear waste storage. The results confirm previous calculations and increase confidence and robustness for future safety assessments.

1 Aim of the study

The aim of this study is to model the transport of radionuclides through the Boom clay, taking into account the geological heterogeneity and the excavation induced fractures around the galleries in which the waste will be stored.

2 Geological context

The safe disposal of nuclear waste is an important environmental challenge. The Belgian nuclear repository program, conducted by ONDRAF/NIRAS, is in the process of characterizing the capacity of the Boom Clay as a natural barrier. At the nuclear zone of Mol/Dessel (province of Antwerp) an underground experimental facility (HADES-URF) was built in the Boom Clay at 225 m depth. In this area, the Boom Clay has a thickness of about 100 m and is overlain by approximately 180 m of water bearing sand formations. Several boreholes provide sets of geological, hydromechanical and geophysical data about the Boom clay.

The Boom clay is a marine sediment of Tertiary age (Rupelian) (Wouters and Vandenberghe 1994). The average hydraulic conductivity value of this formation is very low (K=2.10^{-12} m/s), but the clay is not completely homogeneous. It contains alternating horizontal sublayers of silt and clay with an average thickness of 0.50 m and a large lateral continuity (Vandenberghe et al. 1997). Furthermore, the clay exhibits excavation-induced fractures around the excavated galleries (Dehandschutter et al. 2002). The sublayers have hydraulic conductivity values up to 10^{-10} m/s (Wemaere et al. 2002) and the fractures may have even higher hydraulic conductivity values. These fractures are of a temporary nature as the clay has a considerable "self-healing" capacity.

3 Methodology

To test the robustness of earlier obtained results on the migration of radionuclides in the Boom clay two different approaches were used: a sequential simulation-based (Approach A) and a cokriging-based approach (Approach B). The main characteristics of the methods are summarized in Table 1.

	Approach A	**Approach B**
Dimensionality	1D	3D
Assumptions	horizontal continuity explicitly assumed	horizontal continuity not assumed
Hydraulic conductivity samples	52 K values from borehole A	42 K values from borehole A
Secondary data	- gamma ray of borehole A - resistivity of borehole A - 71 grain size measurements	- resistivity of borehole A - gamma ray of borehole A and B

	- lithology of borehole A	
Analysis and estimation / simulation of K	- data analysis - log transform of K - subdivision of Boom Clay into 3 zones - variogram and crossvariogram fitting - direct sequential simulations with histogram reproduction of hydraulic conductivity - 1D grid in z-direction with 0.2 m interval	- data analysis - no transform of K - no subdivision of Boom Clay - variogram and crossvariogram fitting - 3D cokriging of hydraulic conductivity - 8 by 85 nodes nodes in XYdir on a 25m grid, 1200 nodes in the Z dir on a 0.1m grid (612000 nodes in total)
Fracture simulation	Monte Carlo simulation from distributions based on observed fractures	Monte Carlo simulation from distributions based on observed fractures
Radionuclide	Tc-99	Tc-99
Position of radionuclide source	middle of Boom clay	middle of Boom clay
Hydrogeological model grid	A 20m by 15m by 102m box subdivided into 1m grid nodes in X, 0.17m grid nodes in the in Y and 0.2 to 1m grid nodes in the Z direction	A 100m by 125m by 106m box subdivided into 5m grid nodes in X and Y and 0.1m grid nodes in the Z direction.
Transport program	FRAC3DVS	FRAC3DVS

Table 1. Summary of the two methodologies

4 Data analysis

The value of incorporating the secondary information in the stochastic simulation of hydraulic conductivity was investigated by analyzing correlations between primary and secondary variables (Table 2). All secondary parameters show a fair to very good correlation with hydraulic conductivity and were therefore incorporated in the simulation of hydraulic conductivity.

	Correlation coefficient with hydraulic conductivity	
	Approach A	Approach B
Data	borehole A	borehole A and B
Electrical resistivity	0.73	0.87
Gamma ray	-0.65	-0.73
Grain size (d_{40})	0.95	N/A

Table 2. Correlation coefficients between measured hydraulic conductivity and secondary variables

5 Approach A: simulation of hydraulic conductivity on a 1D grid

5.1 VARIOGRAPHY

Previous geological work (Vandenberghe et al. 1997) on the Boom clay indicated that this formation can be subdivided in three units. For each unit, variograms and crossvariograms were calculated and modeled. The fitted models are given in Table 3. Figure 1a and 1b show two examples of experimental and fitted variograms and cross-variograms: the variogram of gamma ray of the Belsele-Waas Member and the cross-variogram of gamma ray and resitivity of the Belsele-Waas Member.

	Model	Nugget	Range	Sill
Boeretang Member	Spherical	0.035	4.6 m	0.03
Putte and Terhagen Member	Spherical	0.003	4.8 m	0.0056
Belsele-Waas	Spherical	0.23	5.5 m	0.38

Table 3. Fitted log K variograms of the three zones of the Boom Clay formation

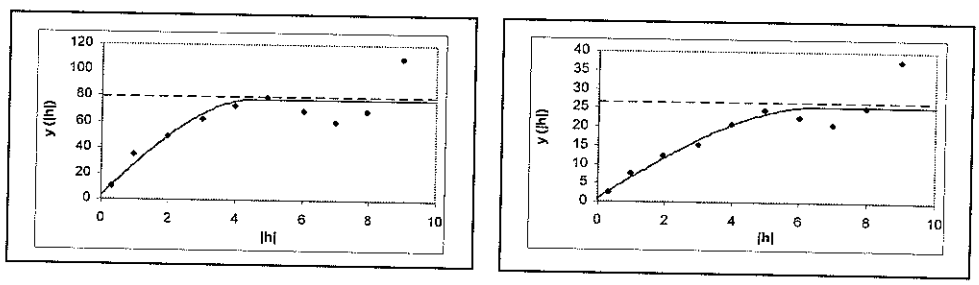

Figure 1. Experimental and fitted a) vertical variogram of gamma ray and b) vertical cross-variogram of gamma ray and resistivity of the Belsele-Waas Member.

5.2 SIMULATION

In this approach, the Boom clay is assumed to be laterally continuous. Therefore, one-dimensional vertical simulations of hydraulic conductivity were calculated on a dense grid in the Z direction (Fig. 2). These hydraulic conductivity values serve as input for the hydrogeological model. The simulation algorithm is iterative and contains the following steps:

1. The location to be simulated is randomly chosen. The spacing between the locations to be simulated was 0.2 m.
2. The simple co-kriging estimate and variance are calculated using the original primary and secondary data and all previously simulated values using COKB3D (Deutsch and Journel 1998).
3. The shape of the local distribution is determined in such a way that the original histogram of hydraulic conductivity is reproduced by the simulation. This is achieved by the following approach. Before the start of the simulation, a look-up table is constructed by generating non-standard Gaussian distributions by choosing regularly spaced mean values (approximately from -3.5 to 3.5) and variance values (approximately from 0 to 2).

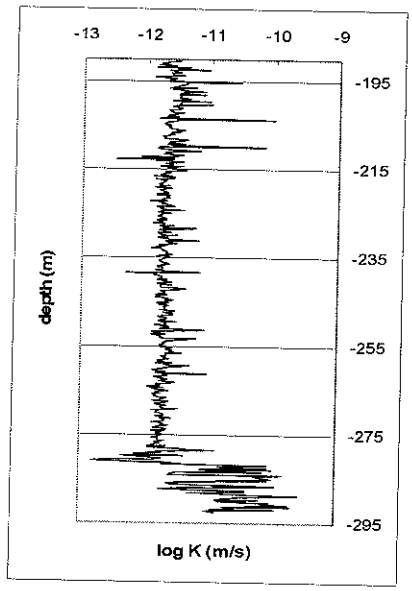

The distribution of uncertainty in the data space can then be determined from back transformations of these non-standard univariate Gaussian distributions by back transformation of L regularly spaced quantiles, p^l, $l=1,...,L$:

$$K^l = F_K^{-1}\left[G\left(G^{-1}\left(p^l\right)\sigma_y + y^*\right)\right], \quad l = 1,...,L$$

where $F_K(K)$ is the cumulative distribution function from the original K variable, $G(y)$ is the standard normal cumulative distribution function, y^* and σ_y are the mean and standard deviation of the non-standard Gaussian distribution and the p^l, $l=1,...,L$ are uniformly distributed values between 0 and 1. From this look-up table the closest K-conditional distribution is retrieved by searching for the one with the closest mean and variance to the co-kriging values (Oz et al. 2003).

Figure 2. Simulation of the vertical hydraulic conductivity of the Boom Clay

4. A value is drawn from the K-conditional distribution by Monte-Carlo simulation and assigned to the location to be simulated. This approach creates realizations that reproduce (1) the local point and block data in the original data units, (2) the mean, variance and variogram of the variable and (3) the histogram of the variable (Oz et al. 2003).

6 Approach B: Estimation of hydraulic conductivity on a 3D grid

In the first approach a perfect horizontal layering was assumed and therefore the hydraulic conductivity values were simulated on a 1D vertical grid. In this approach we assume lateral variability and hydraulic conductivity is estimated on a 3D grid using information from boreholes 2000m apart.

6.1 VARIOGRAPHY

A coregionalization model was fitted to the variograms and cross-variograms. To model the horizontal continuity, gamma ray data are available in two boreholes 2048 m apart. The experimental horizontal variogram was calculated in 30 cm horizontal slices resulting in two average y(h) points, one at the origin and one at the interdistance between boreholes. The model in the horizontal direction has a range of 3 km. Fig. 3 illustrates the automatic sill fittings of the down hole cross-variograms of gamma ray and resistivity and resistivity and hydraulic conductivity.

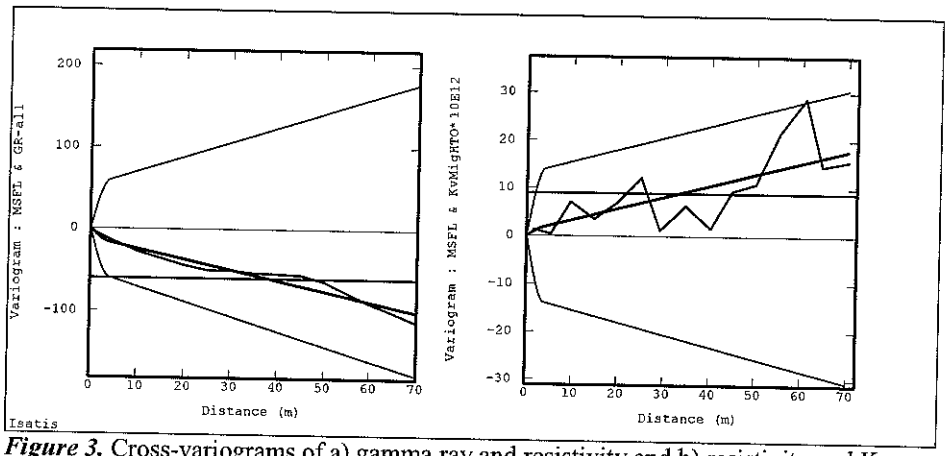

Figure 3. Cross-variograms of a) gamma ray and resistivity and b) resistivity and K.

6.2 ESTIMATION

The estimation is a straightforward cokriging on a 3D grid with a very fine mesh (10cm) in the Z direction. Fig. 4 illustrates one section between the two boreholes. There is more variability on the left side than on the right side of Fig. 4 due to the better conditioning of the co-kriging since the measured hydraulic conductivity values are only available in the borehole on the left.

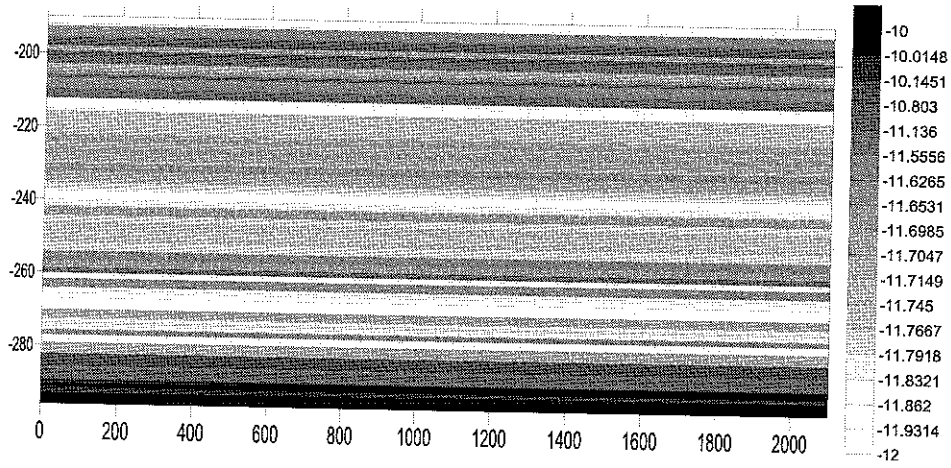

Figure 4. Logarithm of cokriged hydraulic conductivity in an YZ-profile

7 Simulation of fractures

Around the galleries in the Boom Clay, excavation-induced fractures are observed (Fig. 5). The excavation-induced fractures around the future disposal galleries were modeled as discrete fractures. Since these fractures will probably have similar properties to the fractures observed in previously excavated galleries in the Boom Clay, the input

probability distributions of the fracture properties were derived from measurements carried out during recent tunnel excavation in the Boom Clay (Dehandschutter et al. 2002; Dehandschutter 2002; Mertens et al. 2004). These distributions are summarized in Table 4.

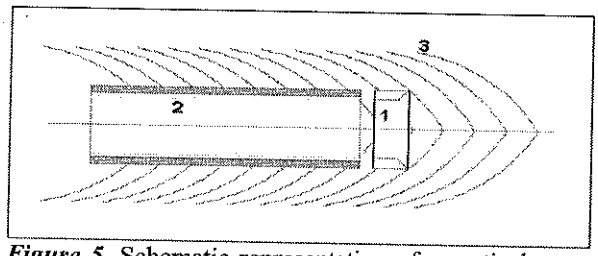

Figure 5. Schematic representation of a vertical cross section through the Connecting Gallery showing the typical symmetrical form of the encountered shear planes (1. Tunneling maching; 2. Supported tunnel; 3. Induced shear planes)

Variable	Distribution
fracture length	uniform distribution U (1m, 3m)
fracture aperture	uniform distribution U (0μm, 50μm)
fracture spacing	normal distribution N (0.7m, $(0.12m)^2$)
fracture dip	normal distribution N (53°, $(11°)^2$)
fracture strike	perpendicular to the excavation

Table 4. Distributions of fractures properties around an excavated zone. The five distributions are assumed uncorrelated and independent.

8 Hydrogeological model

A local 3D hydrogeological model of the Boom Clay, including the estimation/simulations of matrix hydraulic conductivity values and the fractures, was constructed. The boundary conditions, radionuclide and source term model are the same for the hydrogeological models with the 1D K-simulations and the 3D co-kriged K-values. The model size and grid are different for both approaches (Table 1). The size of the model was a compromise between including as many fractures as possible and keeping the computation time manageable. The fine grid resolution in the Z direction was necessary to include the high resolution simulations of hydraulic conductivity and the geometry of the fractures. The vertical boundary conditions for groundwater flow are zero flux boundary conditions since the hydraulic gradient is vertical. Both approaches use the same Dirichlet horizontal boundary conditions. The specified head at the upper boundary is 2 m higher than the specified head at the lower boundary as the upward vertical hydraulic gradient is approximately 0.02 in the 100 m thick Boom Clay (Wemaere and Marivoet 1995). Zero concentration boundary conditions (Mallants et al. 1999) for transport are applied at the upper and lower boundaries of the clay since solutes reaching the boundaries are assumed to be flushed away immediately by advection in the overlying and underlying aquifers.

The model was calculated for the radionuclide Tc-99. Previous calculations revealed that this was one of the most important in terms of dose rates from a potential high-level waste repository for vitrified waste (Mallants et al. 1999). This radionuclide has a half-life of 213,000 years, a solubility limit of 3e-8 mole/l and a diffusion coefficient of 2e-10 m^2/s and a diffusion accessible porosity of 0.30 was assumed for the clay. The transport processes considered in the model are advection, dispersion, molecular diffusion and radioactive decay.

The nuclear waste disposal galleries are assumed to be situated in the middle of the Boom Clay. The radionuclide source is modeled as a constant concentration source with a prescribed concentration equal to the solubility limit. The radionuclides slowly dissolve until exhaustion of the source.

For both approaches the radionuclide migration was calculated using FRAC3DVS, a simulator for three-dimensional groundwater flow and solute transport in porous, discretely-fractured porous or dual-porosity formations (Therrien et al. 1996, Therrien et al. 2003). The fractures were modeled as discrete planes with a saturated hydraulic conductivity of (Bear 1972):

$$K_f = \rho g (2b)^2 / (12\mu)$$

where ρ is the fluid density (kg/m^3), g is the acceleration due to gravity (m/s^2), $2b$ is the fracture aperture (m) and μ is the fluid viscosity (kg/(ms)). The model was run with the different simulations of hydraulic conductivity and fractures as input.

9 Results and discussion

9.1 RESULTS OF APPROACH A

Figure 6 shows the total Tc-99 fluxes through the lower clay-aquifer interface for 10 different simulations.

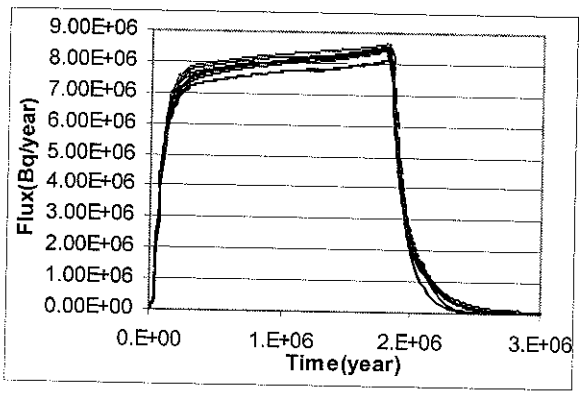

Figure 6. Total Tc-99 flux (Bq/year) through the lower clay-aquifer interface (1Bq = 1 disintegration / sec) calculated with approach A. Tc-99 has a half-life of 213,000 years.

The fluxes through the clay-aquifer interfaces increase relatively fast the first 200000 years. From 200,000 until 1,750,000 years, the fluxes increase more slowly. The fluxes decrease afterwards due to exhaustion of the source. The difference between the fluxes of the 10 different simulations is the largest in the time period from 200,000 till 1,750,000 years. The total amount of Tc-99 leaving the clay was calculated as the flux integrated over time for each simulation. The total Tc-99 masses leaving the clay vary between 1.423e+13 Bq and 1.541e+13 Bq through the lower clay-aquifer interface and between 1.443e+12 Bq and 1.489e+12 Bq through the upper clay-aquifer interface.

9.2 RESULTS OF APPROACH B

The Tc-99 fluxes calculated by this model were 1.45e13 Bq through the lower clay-aquifer interface and 1.38e13 Bq through the upper clay-aquifer interface (Fig.7). The flux through the lower clay-aquifer interface is in the range of fluxes calculated with the model with one-dimensional hydraulic conductivity simulations. The flux through the upper clay-aquifer interface is 4% smaller than the lowest flux calculated with approach A. These fluxes are thus approximately the same as the fluxes calculated by the model with 1-dimensional hydraulic conductivity simulations. This indicates that the assumption of perfect horizontal layering has no large effect on the calculated fluxes.

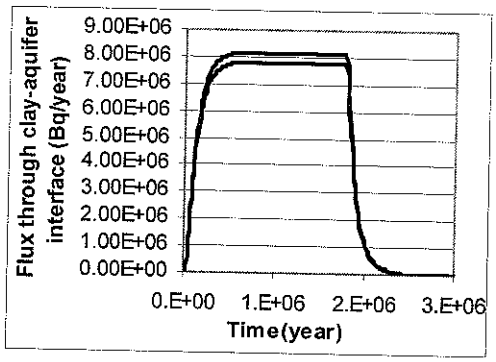

Figure 7. Total Tc-99 flux (Bq/year) through the lower and upper clay-aquifer interface calculated with approach B. Tc-99 has a half-life of 213,000 years.

9.3 DISCUSSION AND CONCLUSION

The range of total Tc-99 masses leaving the clay is rather small. The difference between the largest and the smallest calculated mass leaving the Boom clay is 8%. This result is important for the evaluation of the suitability of the Boom Clay Formation as a host rock for vitrified nuclear waste storage. The total mass fluxes leaving the clay, taking excavation induced fractures and high-conductivity sublayers into account, are not very different from the mass fluxes calculated by a simple homogeneous model. Changes in the modeled heterogeneity of hydraulic conductivity of the clay do not change the output fluxes significantly and therefore do not affect the ability of the clay to store vitrified nuclear waste in the predictive modeling. This again suggests that the Boom clay is a very robust barrier.

Acknowledgements

The Fund for Scientific Research – Flanders provided a Research Assistant scholarship to the first author. We thank ONDRAF/ NIRAS (Belgium agency for radioactive waste and enriched fissile materials) and SCK-CEN (Belgian Nuclear Research Centre) for providing data for this study. We thank René Therrien and Rob McLaren for providing Frac3dvs and for their assistance.

References

Allen D. et al., 1997, How to use Borehole Nuclear Magnetic Resonance. Oilfield Review Summer 1997, pp 34-57.

Bear J., 1972, *Dynamics of fluids in porous media*, American Elsevier, New York

Dehandschutter B., Sintubin M., Vandenberghe N., Vandycke S., Gaviglio P. and Wouters L., 2002, Fracture analysis in the Boom Clay (URF, Mol, Belgium), *Aardk. Mededel.*, 12, 245-248

Dehandschutter B., 2002, Faulting and Fracturing during Connecting Gallery tunnelling at the URL at Mol (SCK-CEN), ONDRAF/NIRAS unpublished internal report

Dehandschutter B., Vandycke S., Sintubin M., Vandenberghe N., Gaviglio P., Sizun J.-P. and Wouters L.,2004, Microfabric of fractured Boom Clay at depth: a case study of brittle-ductile transitional clay behaviour, *Applied Clay Science*, in press

Deutsch C.V. and Journel A.G., 1998, *GSLIB geostatistical software library and user's guide*, Oxford University Press, New York

Mallants D., Sillen X. and Marivoet J., 1999, *Geological disposal of conditioned high-level and long lived radioactive waste: Consequence analysis of the disposal of vitrified high-level waste in the case of the normal evolution scenario*, NIROND report R-3383, Niras, Brussel

Mallants D., Marivoet J. and Sillen X., 2001, Performance assessment of vitrified high-level waste in a clay layer, *Journal of Nuclear Materials*, 298, 1-2, 125-135

Mertens J. and Wouters, L., 2003, 3D *Model of the Boom Clay around the HADES-URF*, NIROND report 2003-02, Niras, Brussel

Mertens J., Bastiaens W. and Dehandschutter B., 2004, Characterization of induced discontinuities in the Boom Clay around the underground excavations (URF, Mol, Belgium), *Applied Clay Science*, in press

Oz, B., Deutsch, C. V., Tran, T. T. and Xie, Y., 2003, DSSIM-HR: A FORTRAN 90 program for direct sequential simulation with histogram reproduction: *Computers & Geosciences*, v. 29, no.1, p. 39-51.

Vandenberghe N., Van Echelpoel E., Laenen B. and Lagrou D., 1997, *Cyclostratigraphy and climatic eustacy, example of the Rupelian stratotype*, Earth & Planetary Sciences, Academie des Sciences, Paris, vol. 321, p 305-315

Wemaere I. and Marivoet J., 1995, *Geological disposal of conditioned high-level and long lived radioactive waste: updated regional hydrogeological model for the Mol site (The north-eastern Belgium model) (R-3060)*, Niras, Brussel

Wemaere, I., Marivoet, J., Labat, S., Beaufays, R. and Maes, T., 2002, *Mol-1 borehole (April-May 1997): Core manipulations and determination of hydraulic conductivities in the laboratory (R-3590)*, Niras, Brussel

Wouters, L. and Vandenberghe, N., 1994, *Geologie van de Kempen: een synthese*: Niras, NIROND-94-11, Brussel

Therrien R. and Sudicky E.A., 1996, Three-dimensional analysis of variably-saturated flow and solute transport in discretely-fractured porous media, *Journal of Contaminant Hydrology*, 23, 1-2, p. 1-44.

Therrien R., Sudicky E.A. and McLaren R.G., 2003, *FRAC3DVS: An efficient simulator for three-dimensional, saturated-unsaturated groundwater flow and density dependent, chain-decay solute transport in porous, discretely-fractured porous or dual-porosity formations, User's guide*, 146 p.